ESPM-17 17th European Solar Physics Meeting ESPM-17
Topic 4 #275
Paper title: Detailed Thermal and Nonthermal Processes in an A-class Microflare
Published in *the Astrophysical Journal*, 930:147 (11pp), 2022 May 10

The imaging evidence of low-energy cutoff

Zhentong Li[1,2]✉, Yang Su[1,2], Astrid M. Veronig[3], Shuting Kong[4,5], Weiqun Gan[1,2], and Wei Chen[1,2]

✉ ztli@pmo.ac.cn
[1] Key Laboratory of Dark Matter and Space Astronomy, Purple Mountain Observatory, CAS [2] School of Astronomy and Space Science, University of Science and Technology of China
[3] Kanzelhöhe Observatory-IGAM, Institute of Physics, University of Graz [4] Institute for Advanced Study, Tsinghua University [5] Cuiying Honors College, Lanzhou University

Abstract

In this poster, I will firstly show the energy release and plasma heating processes in the microflare first reported by Glesener et al. 2020, which shows the existence of a nonthermal component down to 6.5 keV in the X-ray spectrum. Using careful differential emission measure (DEM) analysis and the calculated multithermal X-ray component, we confirm the existence of the nonthermal component in the observed X-ray spectrum. Most importantly, we report the **first imaging evidence for low-energy cutoff** of energetic electrons in EM maps of >10 MK plasma, which first appeared as two coronal sources significantly above the chromospheric footpoints. This study reveals the important role of electron thermalization and low-energy cutoffs in the physical processes of microflares.

Background

The low-energy cutoff E_C of energetic electrons is a key parameter in flare X-ray studies and particle acceleration theories. Since energetic electrons follow a power-law distribution, E_C is the most important factor for determining the total number of electrons, and the total energy carried by the electrons, and it may also carry important information about the acceleration mechanisms. Although the existence of a physical cutoff in the electron distribution is still under debate, there are quite a number of works on the derivations of low-energy cutoffs. The full spectral signature of E_C has been rarely observed in flares.

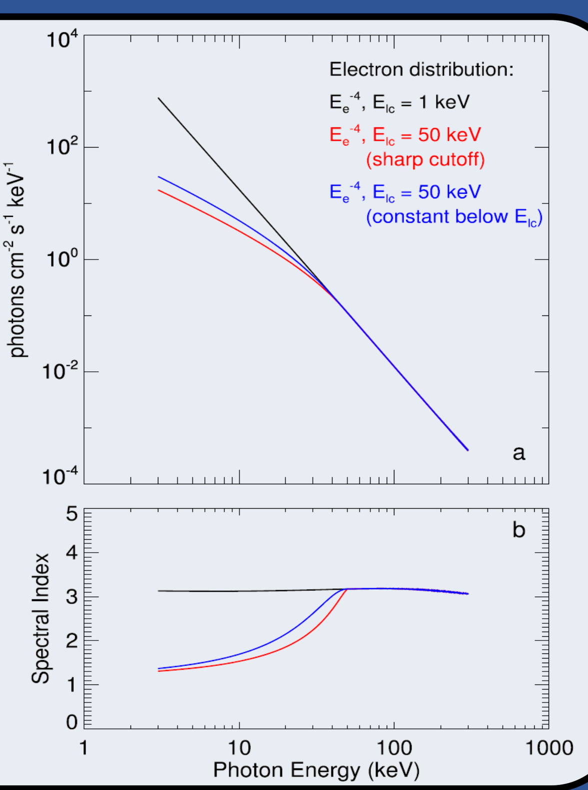

Event Overview

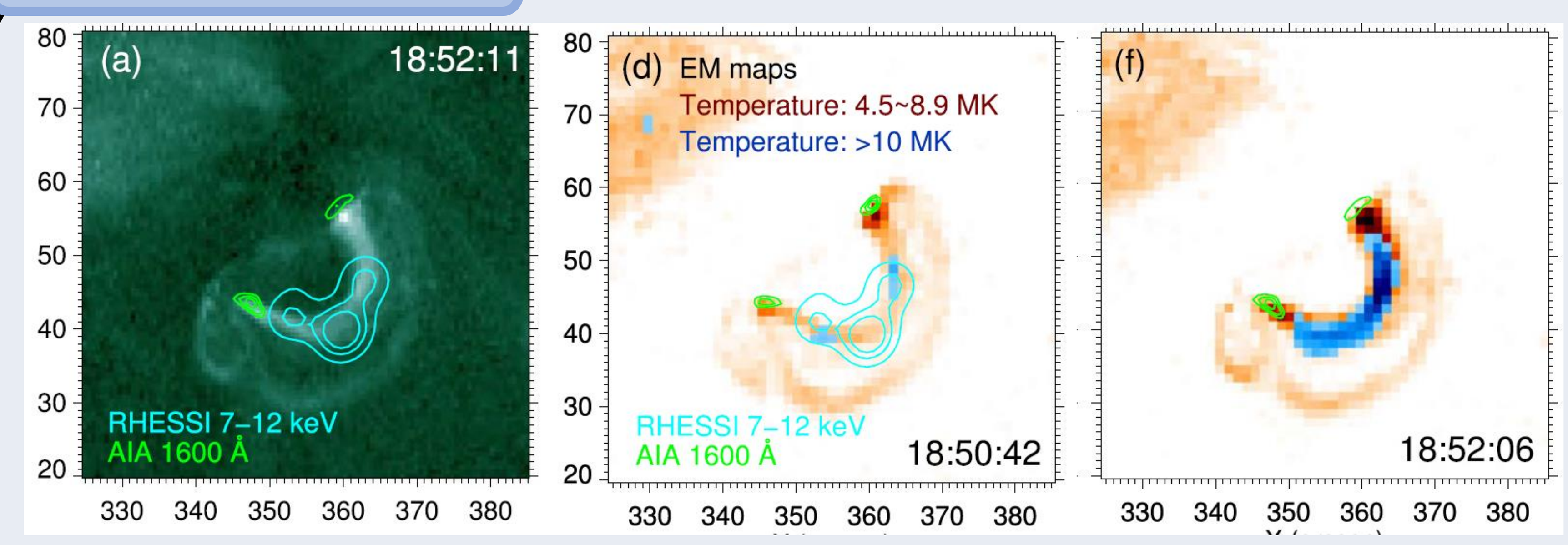

Event date: 2017-08-21 UT
Active region: AR12671

GOES class: A5.7
Center: [355″, 50″]

Notice: the >10 MK sources are away from the chromospheric footpoints.

Evidence of Nonthermal Component

Routine

- DEM → thermal emission photon spectrum → count spectrum
- NuSTAR count spectrum

■ Difference: **nonthermal** component

- spectral fitting: thick target model $\delta \approx$ **6.8**
- nonthermal e⁻ flux: (1.52±0.28)×10^{35} e⁻/s
- low-energy cutoff: (**7.1**±0.5) keV
- energy:
  - deposition rate: ~2.1×10^{27} erg/s
  - total nonthermal energy in 3min: ~**3.8×10^{29}** erg

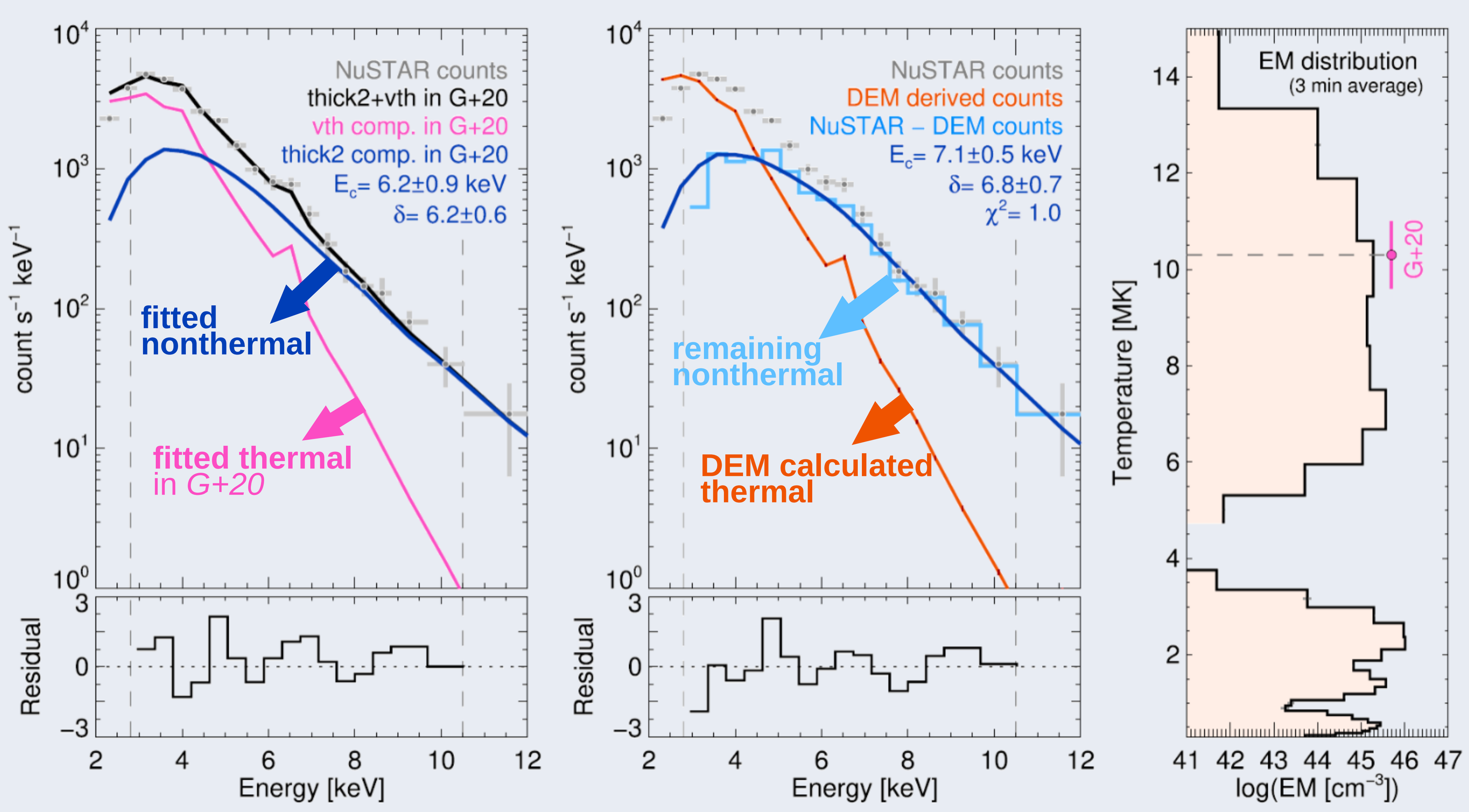

In this work, we used the sparse inversion DEM code, with the improved settings, which better constrain the plasma EM at high temperatures (code available at the end of the poster). We use DEM to constrain the thermal spectrum, then subtract it from the NuSTAR spectrum. The remaining component should be the nonthermal component. We use a thick target model to fit this component and get the parameters of nonthermal electrons in the figure. In this case, the thermal spectrum independently calculated from DEM is in very good agreement with the best-fit thermal component in G20, confirming the existence of a remaining nonthermal component. Note that we also reveal the multitemperature nature of flare plasma, rather than isothermal.

Imaging Evidence of Low-energy Cutoff

Why are the >10 MK sources away from the chromospheric footpoints?
Two possible explanations:

1. Local high density thick target
2. Enough column density and suitable low-energy cutoff

How to check which is correct? Calculate the column density N_s required to stop electrons with an initial energy of E_s, by the formulas on the right.

$$N_s = 1.5 \times 10^{17} E_s^2 \frac{m_e c^2}{E_s + m_e c^2}$$

$$N(p) = \int_0^p n_e \mathrm{d}L = \sum_{i=0}^{p} \sqrt{\frac{\mathrm{EM}_i}{l}} \cdot \Delta L$$

Routine: initial energy of nonthermal electrons E_s → column density $N(p)$ → stopping/thermalization position p

In the first explanation, a low-energy cutoff is not required for producing isolated compact sources rather than elongated ones. We calculated the stopping positions for the electrons with starting energies E_s of 5 keV and 7.1 keV, respectively. It is found that the two curves are clearly separated, meaning that the two populations are stopped at different positions, in contradiction to this scenario.

In the second explanation, electrons with different energies are stopped at different heights. For the steep power-law distribution of injected electrons in this microflare, **the most electrons have energy of E_c**. Given enough column density along the loop, they are **mostly stopped at similar depths**, which can produce the two isolated sources of ~10 MK.

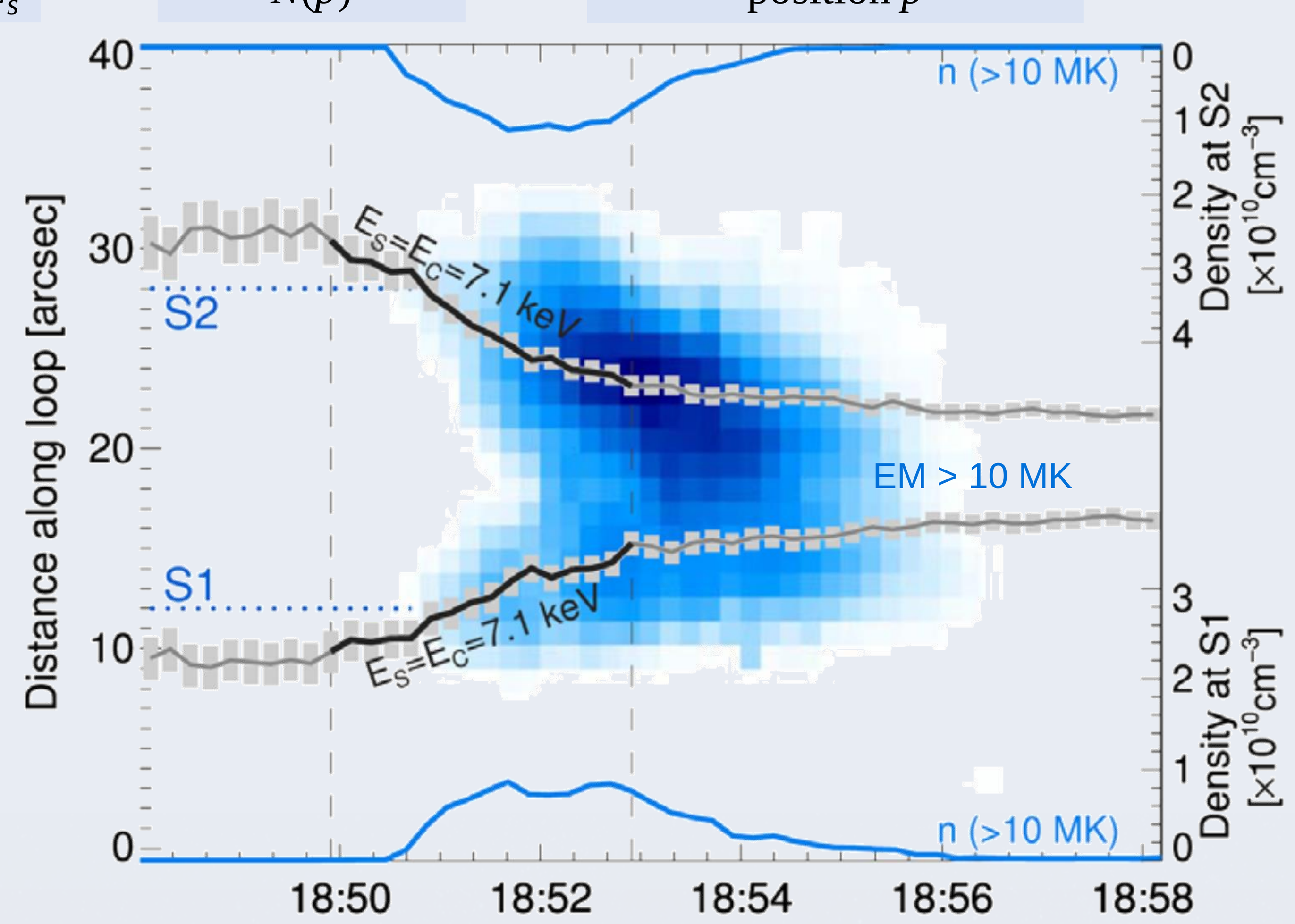

At 18:50:42 UT, when the two >10 MK sources (S1 and S2) appeared, the stopping positions match well with the locations of the two sources, respectively, providing a complete and self-consistent picture of the electron transport with a sharp low-energy cutoff.

Final Model: Beam Heating in the Microflare

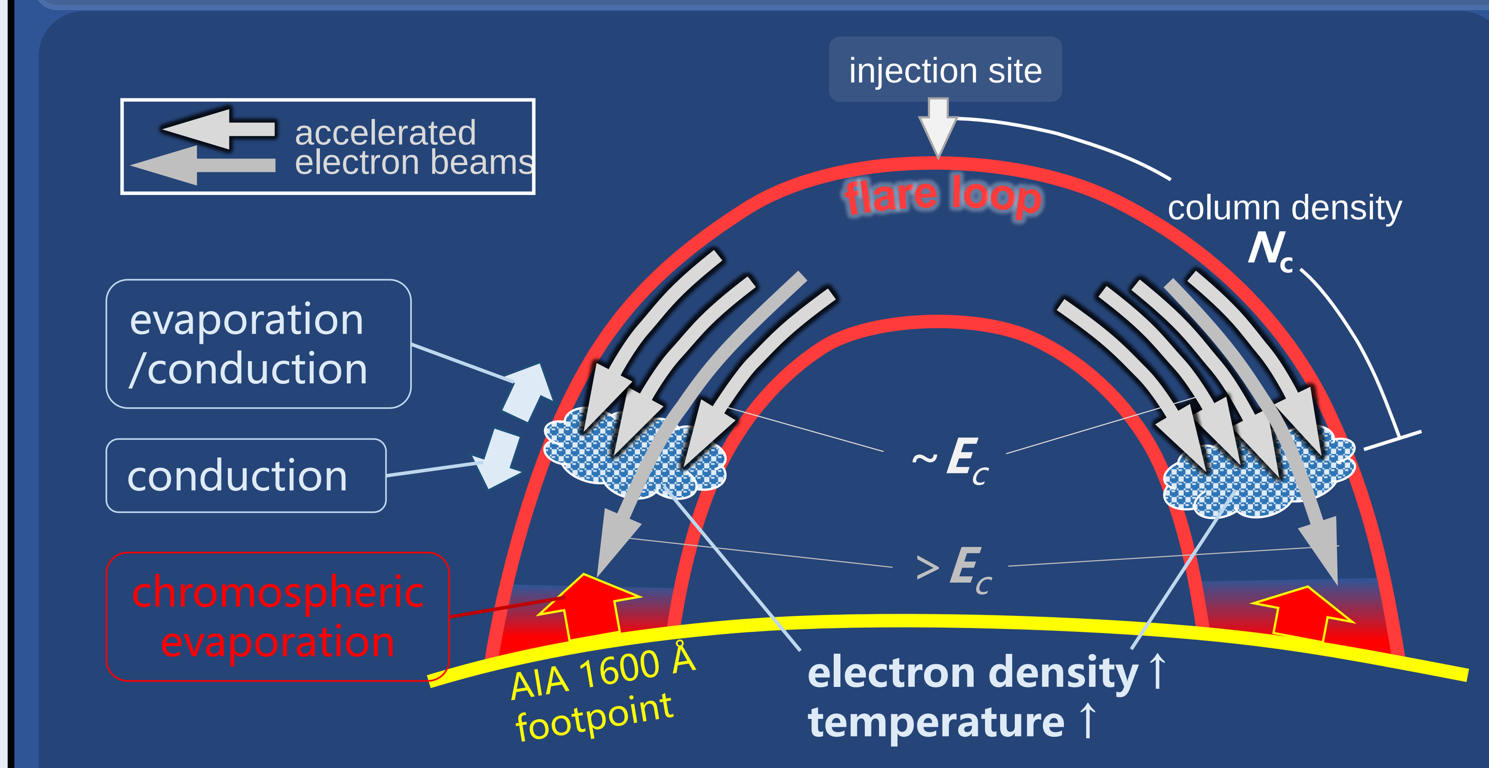

The nonthermal electron beam is injected at the loop top with a low-energy cutoff E_C. N_c is the column density required to stop electrons with energy E_c. Due to the steep spectrum of this microflare, most of the electrons have energies around E_C, they are thermalized due to Coulomb collisions at a similar height in the corona, high above the footpoints, resulting in hot and dense thermal sources. The sources may expand through thermal conduction and/or evaporation.

Summary

- Newly improved sparse DEM code
- Evidence of **nonthermal** emissions in a microflare
- **Multi-thermal** nature of the microflare plasma
- **First imaging evidence** of low-energy cutoff of nonthermal electrons

➢ The research methods in this study provide valuable approach to discover or confirm the nonthermal emissions in microflares.

Download the DEM code   View the article of this work

This work is supported by the National Natural Science Foundation of China (grant Nos. 11820101002, U1631242, 11921003, U1731241, 41774183, 41861134033, and U1931138) and the Strategic Pioneer Program on Space Science, Chinese Academy of Sciences (grant Nos. XDA15320300, XDA15016800, XDA15320104, and XDA15052200).

The spectral cross-calibration of ASO-S/HXI

Zhentong Li[1], Yang Su[1,2] ✉, Wei Liu[1], Wei Chen[1,2], Fu Yu[1], and Weiqun Gan[1,2]

✉ ztli@pmo.ac.cn yang.su@pmo.ac.cn

The importance of cross-calibration: **X-ray directivity**, **3D property of X-ray sources**

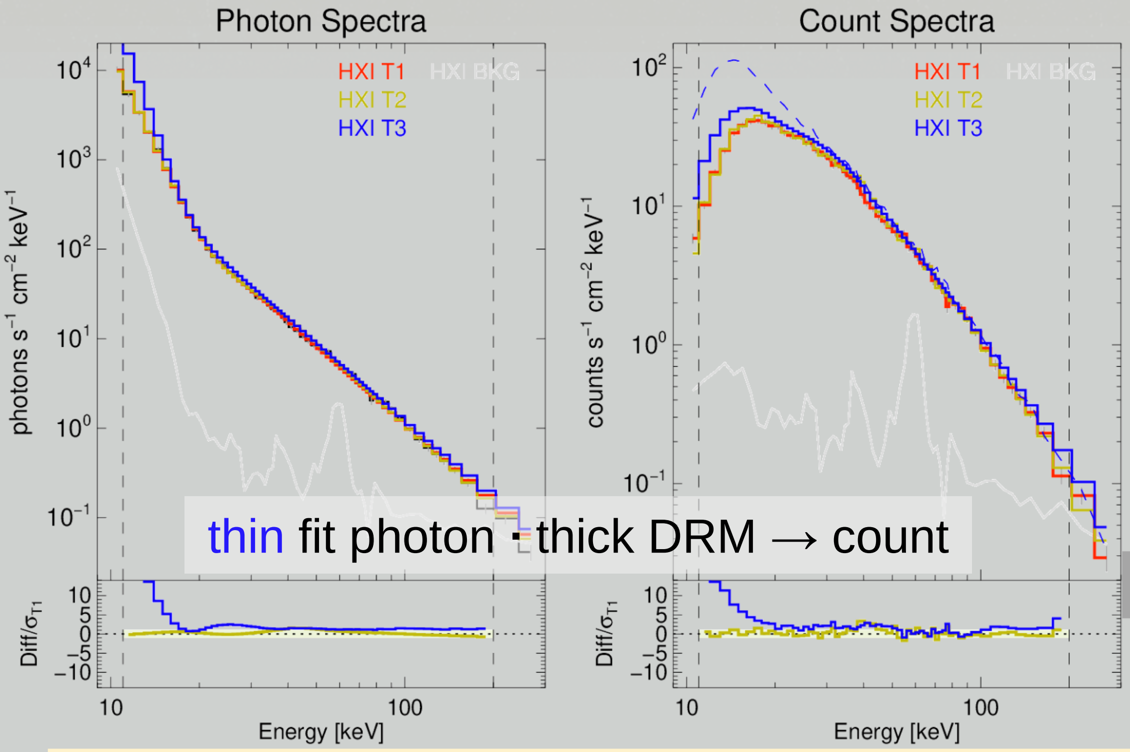

HXI total flux detectors D92(T1) D93 (T2) D94 (T3)

covered by **thick** Aluminum

thin Al

different response

discrepancy between T3 (0.6 mm Al) and **T1, T2**

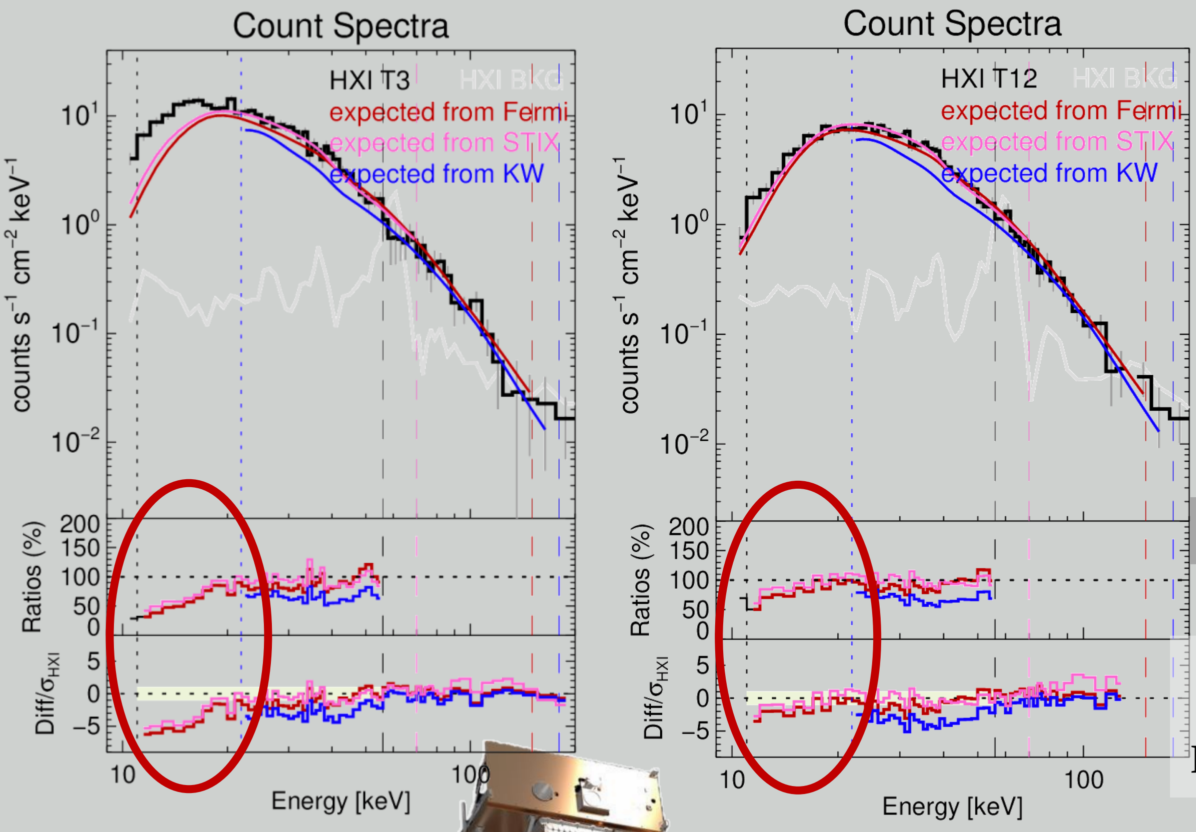

Compare with STIX, Fermi and Konus-Wind data

- f_vth+thick2
- Albedo effect considered

T1+T2 is better than T3

The response of T3 needs to be adjusted

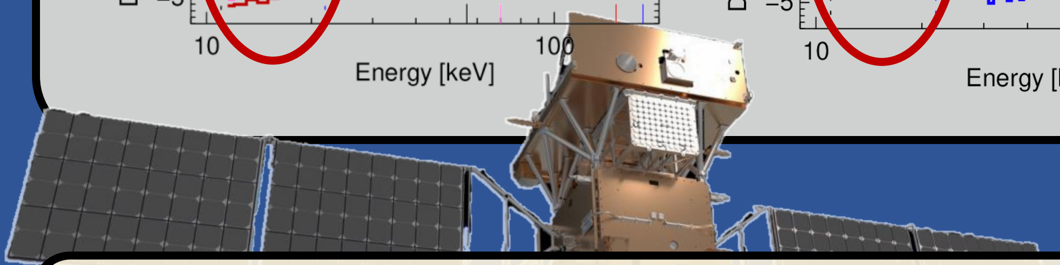

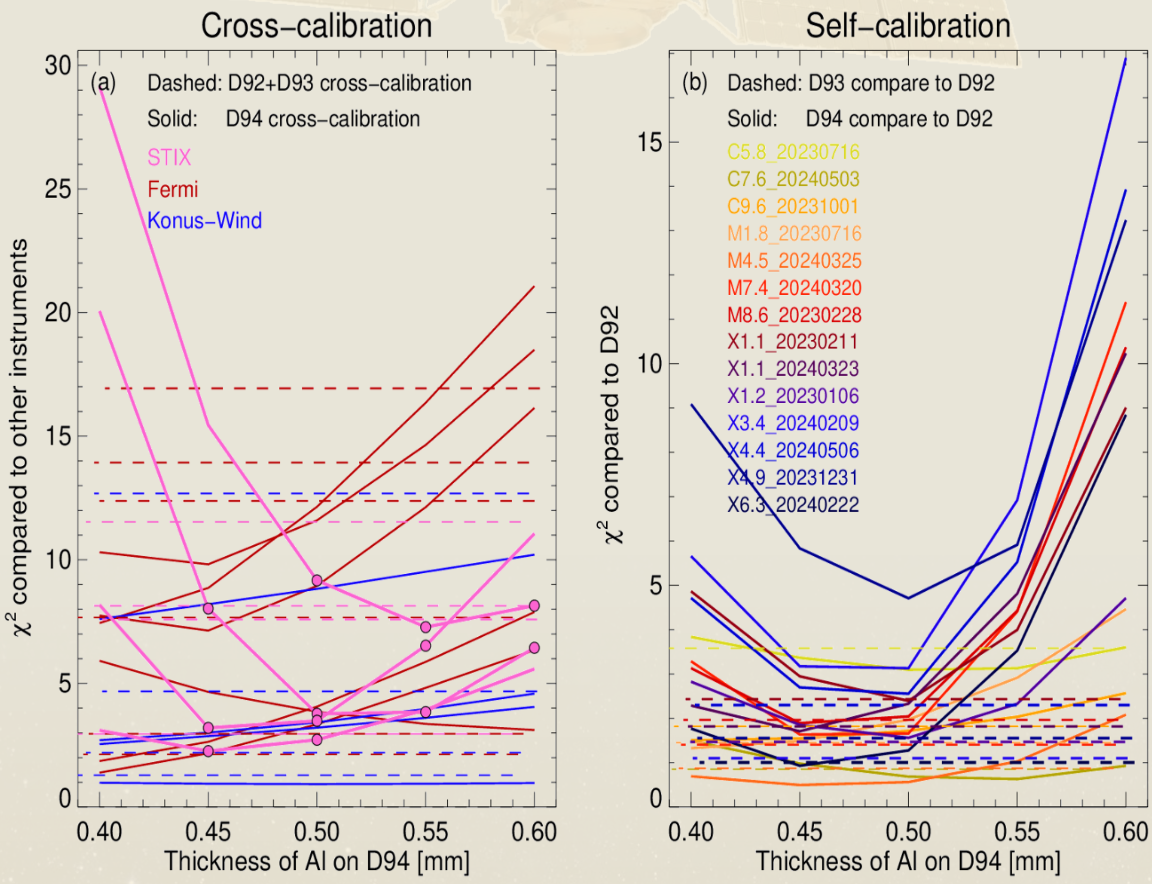

Testing T3 response by changing Al thickness

- GEANT4 simulation
- Dashed lines: **acceptable level**
- D92 (T3) need to change its response using 0.50 mm effective Al thickness
- New response will be released by the next version of HXI GUI